Central European Journal of Energetic Materials
ISSN 1733-7178; e-ISSN 2353-1843

Cent. Eur. J. Energ. Mater., 2016, *13*(4), 989-1004; DOI: 10.22211/cejem/61496

Influence of Processing Techniques on Mechanical Properties and Impact Initiation of an Al-PTFE Reactive Material

Bin FENG,* Xiang FANG, Yu-Chun LI, Shuang-Zhang WU, Yi-Ming MAO, Huai-Xi WANG

PLA University of Science and Technology
88 Hou Biao Yiing Road, Qin Huai District, 210007 Nanjing, China
**E-mail: fengbin.plaust@foxmail.com*

Abstract: Reactive materials (RMs) or impact-initiated materials have received much attention as a class of energetic materials in recent years. To assess the influence of processing techniques on mechanical properties and impact initiation behaviors of an Al-PTFE reactive material, quasi -static compression tests and drop-weight tests were performed. Scanning electron microscopy (SEM) was used to identify the characteristics of the interior microstructures of the Al-PTFE samples. A sintering process was found to transform Al-PTFE from a brittle to a ductile material with an increased elasticity modulus (from 108-160 MPa to 256-336 MPa) and yield stress (from 12-16 MPa to 19-20 MPa). Increasing the molding pressure from 36 MPa to 182 MPa increased the elastic modulus of all Al-PTFE samples and also the yield stress of unsintered ones. Unsintered samples in general required less energy to initiate than sintered ones. As the molding pressure increased, the impact initiation energy for sintered Al-PTFE fell from 96 J to 68 J, whereas the initiation energy for unsintered Al-PTFE rose from 68 J to 85 J. PTFE nanofiber networks observed in sintered samples formed under the higher molding pressures could contribute to the opposite trends observed in the impact initiation energy of unsintered and sintered Al-PTFE samples.

Keywords: Al-PTFE, reactive materials, quasi-static compression, impact initiation

1 Introduction

Reactive materials (RMs) or impact-initiated materials have received much attention as a class of energetic materials in recent years. They offer higher

energy densities than the best existing monomolecular energetic materials by a factor or two [1]. RMs can be combinations of thermites, intermetallics, metal/polymer mixtures, metastable intermolecular composites (MICs), matrix materials, as well as hydrides [2]. Of all the different types of RMs, mixtures of Al and PTFE (polytetrafluoroethylene) have been extensively studied, because of their large heat of reaction and the favorable combinations of properties of that PTFE exhibits such as low friction coefficient, high thermal stability, high electrical resistance, high chemical inertness, high melting point and easiness of forming [3]. Al-PTFE has many possible military and civilian uses such as structural reactives for damaging targets or as an additive to propellant/explosive mixes, in which a certain degree of mechanical strength is needed. Thus a processing procedure which includes mixing of constituents, pressing the mixture to nearly theoretical maximum density (TMD) and sintering [4-6] is often adopted to enhance the integrity of Al-PTFE pellets, rods or charge liners during normal transport and also under launch acceleration. Therefore, to understand the interaction between the mechanical properties of strengthened RMs and their reaction performance under compression is of great importance.

The taxonomy proposed by Thadhani [7] is often used to explain the reaction mechanisms of RMs [8-10]. This taxonomy classifies solid-state chemical reactions in power mixtures into shock-induced (mechanochemical process controlled) or shock-assisted (thermochemical process controlled) reactions. For impact initiation of strengthened Al-PTFE, the shock-induced reaction is unlikely to occur because of (i) the relatively long ignition time (usually on the order of tens of microseconds [11]) for strengthened Al-PTFE compared with that of shock-induced reaction (normally tens to hundreds of nanoseconds [12]), and (ii) the lack of a "crush-up" process of power mixtures which is assumed to be related to the mechanism of shock-induced reaction [12]. On the other hand, it is generally accepted that the initiation of pressed Al-PTFE is a strong function of heating rate. When impacted at speeds ranging from 200 m/s to 5000 m/s, the material first undergoes a plastic deformation and flow or a fracture process that causes intimate mixing of the constituents, then diffusion controlled ignition takes place at heating rates ranging from 10^4 K/s to 10^8 K/s [13]. It is also believed that large strain deformations, shear bands and fractures formed during the impact play a significant role in the initiation of Al-PTFE, which could be supported by the phenomenon observed by Ames [14] and Lee *et al*. [15] during two-step impact experiments where the majority of the reaction appeared to occur following material breakup and subsequent impact on a hardened steel anvil. However, the mechanism of impact-initiated reaction of strengthened RM is still not fully understood, because complex processes such as chemical

reaction and plastic flow cannot be directly observed with current technology. However, it is still safe to say that the processing techniques of densely pressed RM solids could affect their mechanical response under compression, thereby influencing the impact initiation behavior.

To explore the mechanical property of strengthened Al-PTFE, numerous experiments have been conducted by different research groups. Casem [16] used quasi-static compression and split Hopkinson bar (SHPB) tests to investigate the mechanical response of pressed and sintered Al-PTFE rod (Al: 26.5 wt.%, 44 μm; PTFE: 73.5 wt.%, 31 μm) over strain rates ranging from 0.001/s to 9000/s and temperatures ranging from 295 K to 351 K. The data collected was applied to generate parameters for constitutive models including the Johnson/Cook (JC) model, the Modified Johnson/Cook (MJC) model, and the Zerilli/Armstrong (ZA) model for polymers. Similar experiments were carried out on sintered Al-PTFE cylinders (Al: 26 wt.%, 9 μm; PTFE: 74 wt.%, 28 μm) by Raftenberg *et al*. [17] at a strain rate of 0.1/s and 2900/s. On the basis of these data, a fit to the JC model was obtained with different parameters compared with Casem's results. To increase the density and the strength of the RM, tungsten (W) can be added into Al-PTFE mixtures. Cai *et al*. [3, 18] made a detailed study of the mechanical properties of unsintered Al-PTFE/W rod by using quasi-static tests, SHPB and drop-weight experiments, while Xu *et al*. [19] tested the tensile strength and fracture energy of pressed and sintered Al-PTFE/W [20]. However, the studies mentioned above have been mainly focused on the mechanical properties of strengthened Al-PTFE, so the relation of these properties to impact initiation behavior was not well explained. Furthermore, it is important to notice that intrinsic properties (such as density, sound speed and yield strength) and/or extrinsic properties (such as particle morphology and initial density) of RM constituents, as well as processing techniques, could be quite different in different laboratories, which would change the mechanical properties of strengthened RMs and alter their impact initiation behavior.

The purpose of this study was to explore the interaction between mechanical properties and impact initiation behavior of Al-PTFE by altering steps in the processing technique such as pressing and sintering. Although a considerable number of experiments have been focused on the influence of intrinsic properties and/or extrinsic properties of constituents on the impact initiation behavior of RMs [12, 13, 21-23], the pressing and sintering processes have not received as much research attention. However, once the constituents of an RM mixture are chosen, pressing and sintering become major factors that influence the sample strength which in turn controls the plastic deformation and breaking up processes, both of which have a major effect on the impact initiation and reaction behavior.

That makes processing techniques crucial to the design and control of RMs in application.

2 Experimental

2.1 Sample preparation

A preparation process was adopted similar to that of Nielson *et al.* [4] which included mixing, cold pressing and sintering. The average diameters of the initial powders were: Al: 6-7 μm (JT-4, Hunan); PTFE: 25 μm (3M, Shanghai). All samples were fabricated using the same batch of purchased powders. Therefore the characteristic differences between different batches of materials provided by a given producer, which had been reported by Yarrington [24], were minimized.

Al and PTFE powders (26.5 wt.%/73.5 wt.%) were suspended in an ethanol solution and mixed using a motor-driven blender for 20 min. The suspensions were then sonicated for a further 10 min to break up agglomerates. After mixing and sonication, the wet mixtures were placed in a vacuum drying oven for 48 hours at 50 °C. Then a screening stage was used in which the agglomerates were pressed through an 80 mesh screen by hand, to increase the homogeneity of the powders in the pressing stage.

The size of the pressed cylinders was Ø10 mm × 15 mm for quasi-static tests (see Figure 2a) and Ø10 mm × 3 mm for drop-weight tests (see Figure 6a).

A sintering process under vacuum was performed to further strengthen the pressed Al-PTFE samples. Detaileds of this process can be found in Nielson *et al.* [4]. The oven temperature was ramped up to 380 °C at a rate of about 50 K/h. The pressed fragments were held at about 380 °C for 6 h, then the temperature was reduced to 310 °C at a rate of about 50 K/h and held at this temperature for 4 h. The fragments were subsequently cooled to ambient temperature at an average cooling rate of 50 K/h. Half of the samples did not go through the sintering process in order to be able to make a comparison of the mechanical properties and impact initiation behavior of sintered and unsintered Al-PTFE.

2.2 Quasi-static compression tests

Quasi-static compression tests were performed using a DSN100 universal testing machine. The load was applied at the speed of 2 mm/min (equivalent to a nominal strain rate of 0.002/s) for all tested samples and terminated when the sample was fractured. The fracture criterion was determined by when the test machine detected that the compression force had decreased to less than 50%

of the maximum force experienced. The bottom and top of the samples were lubricated with oil to alleviate the buckling phenomenon.

Sintered and unsintered samples prepared under molding pressures ranging from 36 MPa to 182 MPa were divided into 10 groups. For each group 5 samples were tested and stress-strain curves were recorded.

2.3 Drop-weight tests

Drop-weight tests were performed using a fall hammer impact sensitivity tester with a drop mass of 10 kg and a maximum drop height of 1.5 m. Each test was conducted with the sample placed on the center of an anvil without constraint and directly impacted by the drop mass. The anvil is composed of two cylindrical segments, the lower segment having a diameter of 50 mm and the upper segment having a diameter of 30 mm (see Figure 6a). The whole anvil is made of hardened steel to minimize the possible influence of anvil deformation on experimental results. The lower part of the drop hammer is a cylinder with the same diameter as the upper segment of the anvil. A standard Bruceton method was adopted to calculate the drop height that would trigger chemical reactions with a 50% possibility. The ignition energy can then be approximated as the potential energy of the drop weight. High-speed photography with a frame rate of up to 6,000 frames/s was used to observe the impact process. During each test, if the camera had captured any flame, the sample was considered reacted, and vice versa. The impact initiation energy was estimated by the potential energy of the drop mass as in Equation 1

$$E_{ad} \approx E_p = mgh \tag{1}$$

where E_{ad} is the estimated impact initiation energy, E_p is the potential energy of the drop mass, m is the mass of the drop hammer and h is the drop height.

A total of 250 samples were prepared according to different processing techniques and then split into 10 groups. For each group, 25 samples were tested to determine the impact initiation energy.

2.4 Scanning electron microscopy

Samples prepared according to different processing procedures were examined and analyzed using a Hitachi S-3400N II scanning electron microscope (SEM). To identify the characteristics of the interior microstructures of the samples, brittle fracture must be introduced to generate clear cross-sectional surfaces for observation. Because of the great ductility of sintered Al-PTFE, sintered samples were immersed in liquid nitrogen for 5 min before being fractured using pliers.

3 Results and Discussion

3.1 Effect of processing techniques on mechanical properties

Samples that were cold pressed under molding pressures ranging from 36 MPa to 182 MPa (with or without sintering) were subjected to quasi-static compression testing. For each type of sample produced using a specific processing procedure, the elasticity modulus and the yield stress were calculated and averaged from 5 samples. Because of the great ductility of sintered samples compared with unsintered samples, their yield stresses cannot be calculated in the same manner as can be seen from the following analysis. For sintered samples, the yield stress was calculated as the offset yield stress at 2% strain. For unsintered samples, it was calculated as the upper yield stress. All these results and standard deviations are listed in Table 1.

Sintering is a process in which multiple physical changes take place, such as melting, phase transformations and molecular chain realignment. After pressing, many of the PTFE powder particles touch one another, while pores and voids still exist between them. As sintering progresses, when the temperature rises above 588 K, PTFE particles gradually transform from a crystal to an amorphous phase and melt together into a continuous matrix. When cooling through the melting temperature, recrystallization sets in and the strength and toughness of the PTFE matrix are enhanced. The driving force for sintering is the reduction in the total particle surface area as surface energies are larger in magnitude than grain boundary energies [25].

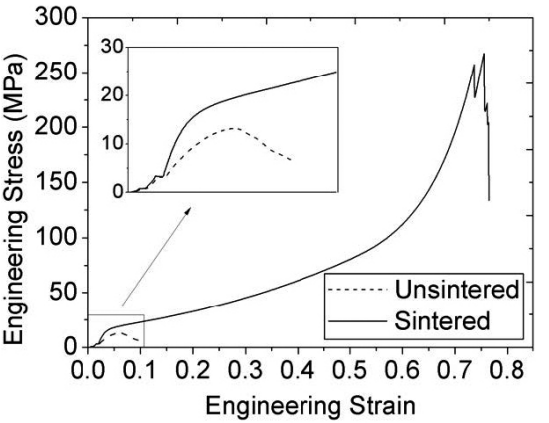

Figure 1. Typical stress-strain curves of unsintered and sintered Al-PTFE.

Table 1. Results of quasi-static compression tests and drop-weight tests, each number was averaged from 5 tested samples for quasi-static compression test and 25 tested samples for drop-weight tests

Molding Pressure [MPa]	Sintering	Density [g/cm^3]	Standard deviation [g/cm^3]	Elasticity modulus [MPa]	Standard deviation [MPa]	Yield stress[a] [MPa]	Standard deviation [MPa]	Impactin itiation energy[b] [J]	Standard deviation [J]
36	YES	2.26	0.06	256	25	19.4	1.2	96.34	1.22
72	YES	2.29	0.06	269	18	19.2	0.9	91.43	1.28
108	YES	2.30	0.04	324	17	19.1	1.0	89.37	1.23
144	YES	2.34	0.04	333	16	20.2	0.4	83.24	1.15
182	YES	2.31	0.05	336	17	19.3	0.5	77.81	1.07
36	NO	2.09	0.05	108	10	12.3	1.0	68.75	1.20
72	NO	2.25	0.04	135	8	13.1	0.8	70.95	1.19
108	NO	2.28	0.05	146	6	15.8	0.7	75.36	1.21
144	NO	2.29	0.03	153	8	16.1	0.5	79.51	1.20
182	NO	2.30	0.03	160	7	17.1	0.6	85.36	1.21

[a] For sintered samples, the yield stress was calculated as offset yield stress at 2% strain. For unsintered samples, the yield stress was calculated as the upper yield stress.

[b] Estimated by the potential energy of the drop mass at the drop height that would trigger chemical reactions with 50% possibility.

Sintering introduced remarkable changes to the mechanical properties of Al-PTFE, as can be seen from Figure 1. During compression, the unsintered sample showed clear evidence of brittleness. The sample first underwent elastic deformation until the yield stress was reached (12-17 MPa); then the stress diminished quickly as the strain increased. The maximum strain that can be borne by the sample before the appearance of axial and shear cracks was between 0.10 and 0.12 (see Figure 2e and 2f). By contrast, sintered samples showed great ductility. A short elastic region was followed by a very long plastic region until the strain reached 0.72 at which point axial cracks appeared caused by the circumferential tensile stress due to the large plastic deformations along the periphery of the cylinder (see Figures 2b-2d). As shown in Figure 3, the elastic moduli of Al-PTFE samples were in general doubled after sintering (increasing from 108-160 MPa to 256-336 MPa). The yield stresses were also increased by sintering, although by a smaller amount (see Figure 4 where the yield stress can be seen to increase from 12-16 MPa to 19-20 MPa).

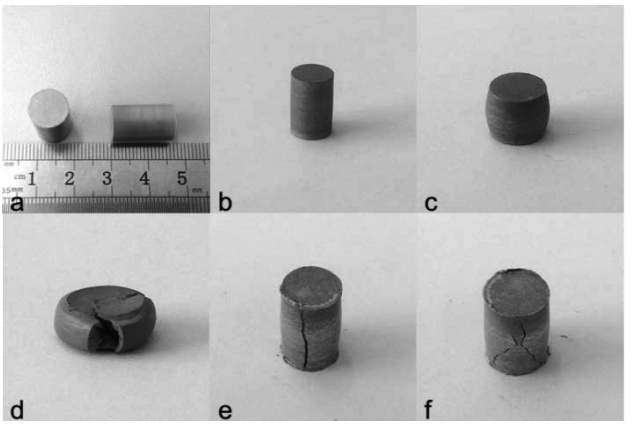

Figure 2. Sintered and unsintered Al-PTFE before and after quasi-static compression: (a) before compression; (b) sintered Al-PTFE at a strain of 0.12; (c) sintered Al-PTFE at a strain of 0.5; (d) sintered Al-PTFE at a strain of 0.72, axial cracks can be seen; (e) unsintered Al-PTFE at a strain of 0.12, axial cracks can be seen; (f) unsintered Al-PTFE at a strain of 0.12, axial and shear cracks can be seen.

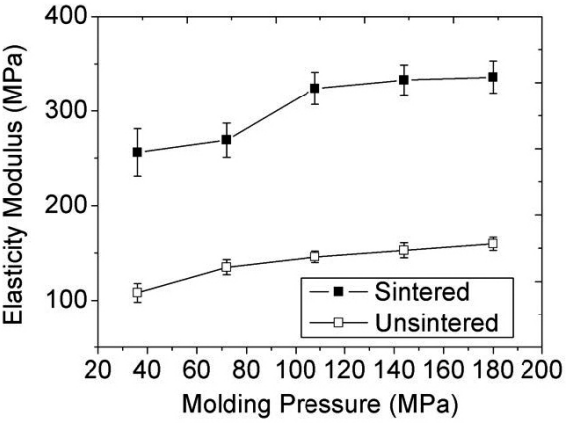

Figure 3. Plot of the elasticity modulus of sintered and unsintered Al-PTFE against molding pressure (data points are average values from 5 independent tests ± the standard deviation).

The molding pressure affects the elasticity modulus and the yield stress of Al-PTFE in different ways. The elasticity modulus increased with increasing molding pressure for both sintered and unsintered samples (see Figure 3). On the other hand, a higher molding pressure caused higher yield stress in unsintered

samples, but the yield stress for sintered samples stabilized at 19-20 MPa which approximates the upper limit of yield stress for PTFE [25] (see Figure 4).

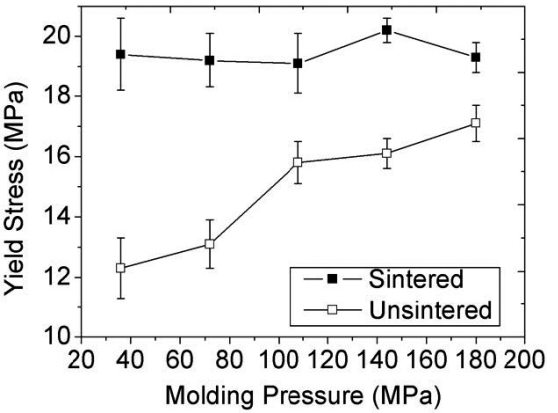

Figure 4. Plot of yield stress of sintered and unsintered Al-PTFE against molding pressure (data points are average values from 5 independent tests ± the standard deviation).

The reasons behind the phenomena described above can be explained by the strength of the PTFE matrix and the interaction between the PTFE matrix and Al particles, as can be observed using scanning electron microscopy. Figure 5 shows the interior microstructures of sintered and unsintered Al-PTFE pressed separately under pressures of 36 MPa and 182 MPa. It can be seen clearly from all the SEM images that spherical Al particles are surrounded by PTFE. PTFE forms the continuous matrix in which the Al particles are discretely distributed.

Figure 5a shows the interior microstructures of unsintered Al-PTFE pressed at 36 MPa, in which the PTFE matrix has the lowest integrity because of the lower molding pressure. The many microcracks in the PTFE matrix indicate weak adhesion between PTFE particles. Multiple PTFE fibers were generated during the compression, but most of the fibers hang loosely and provide little support for the matrix or the Al particles. The interfaces between Al particles and the PTFE matrix are also the weakest in Figure 5a, as can be seen by the obvious crevices between Al particles and the PTFE matrix wrapped around them.

Figure 5b shows unsintered Al-PTFE pressed at 182 MPa, in which PTFE particles were pressed densely and microcracks previously observed in the PTFE matrix disappeared. It is very likely that stronger PTFE fibers were generated and stretched, which means these fibers could bear forces and play a supportive role in the structure. No obvious crevices between Al particles and the PTFE matrix can be observed.

Figure 5c shows sintered Al-PTFE pressed at 36 MPa, in which PTFE particles were fully integrated into one matrix after melting and recrystallization, and Al particles are firmly embedded into the PTFE matrix. Under this low molding pressure, no PTFE fibers can be observed, which may be because loose fibers (seen, for example, in Figure 5a) were fused together into the matrix during the sintering process. Spherical holes observed in the image were created by Al particles that had been pulled out during the fracture.

Interestingly, for sintered Al-PTFE pressed under a higher molding pressure (see Figure 5d), a dense network of PTFE fibers can be observed. Such fibers were also observed by Cai *at al*. [18]. Tens of PTFE nanofibers (diameters as low as 60-200 nm) were attached to each Al particle. These fibers could effectively protect Al particles from being pulled out from the PTFE matrix as happened at the lower molding pressure.

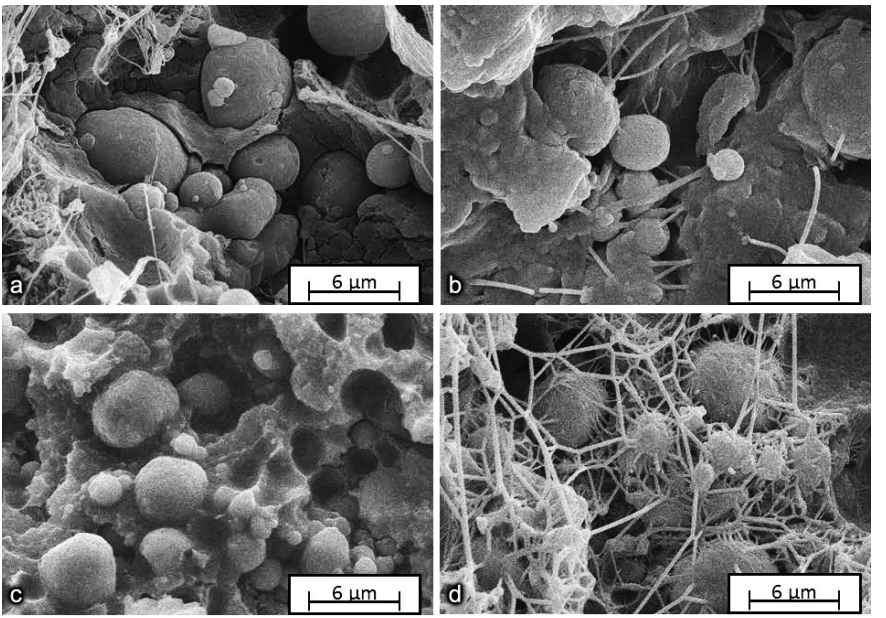

Figure 5. SEM images of the interior microstructures of Al-PTFE produced by different processing procedures: (a) unsintered Al-PTFE pressed under 36 MPa; (b) unsintered Al-PTFE pressed under 182 MPa; (c) sintered Al-PTFE pressed under 36 MPa; (d) sintered Al-PTFE pressed under 182 MPa.

As a composite material, the deformation and failure process of Al-PTFE is controlled by two factors: (i) the interface strength between Al particles and

the PTFE matrix and (ii) the strength of the PTFE matrix itself. The interfacial strength between Al particles and the PTFE matrix could be improved by sintering and/or by increasing the molding pressure. On the question of the PTFE matrix, although increasing the molding pressure could improve the integrity of the PTFE matrix for unsintered PTFE, sintering could improve the integrity more effectively. This statement can be confirmed by making a comparison between Figure 5a and Figure 5c. Notice that the PTFE matrices in Figure 5a and Figure 5c were pressed under the same molding pressure (36 MPa), but after sintering, all microcracks in the PTFE matrix and crevices between Al particles and the PTFE matrix that appeared in Figure 5a disappeared and fused together firmly. During the elastic deformation stage, both the strength of the PTFE matrix and the strength of interfaces between Al particles and PTFE contribute to the elasticity modulus. Therefore, the increase of elasticity modulus could be attributed to the sintering process as well as the higher molding pressure. When the material begins to yield, since the yield stress for aluminum is much higher than that of PTFE (80-100 MPa as compared to 19-20 MPa), the yield process of Al-PTFE mainly occurs in the PTFE matrix. Therefore, the yield stress of an Al-PTFE composite is dominated by the yield stress of the PTFE matrix. After sintering, the yield stress of PTFE reached its upper limit, regardless of changes in the molding pressure. Therefore a higher molding pressure could cause a higher yield stress in unsintered Al-PTFE, whereas the yield stress for sintered Al-PTFE stabilized at 19-20 MPa.

3.2 Effect of processing techniques on impact-initiated reaction behaviors

As shown in Figure 6b, when an Al-PTFE sample was impacted by the drop mass, intense light was produced which was captured by high speed photography. The light is a sign of deflagration or explosion. It can be seen from the recovered sample (see Figure 6c) that the start of reaction was near the edge of the sample where shear deformation concentrates most intensely (a similar reaction pattern reaction has been observed by Ames [14] and Lee *et al*. [15]). Then the reaction propagated from the edge to the center of the sample and quenched. We attribute the quenching to the rapid densification caused by the drop mass, since constrained space would limit further shear deformation in the central region of the sample.

Impact initiation energy and standard deviations derived from drop-weight tests for Al-PTFE prepared by different processing techniques are listed in Table 1 and plotted in Figure 7. It can be seen from Figure 7 that unsintered samples in general required less energy to initiate than sintered samples, except samples

pressed at 182 MPa. Interestingly, the initiation energy for sintered Al-PTFE fell from 96 J to 68 J, whereas the initiation energy for unsintered Al-PTFE rose from 68 J to 85 J.

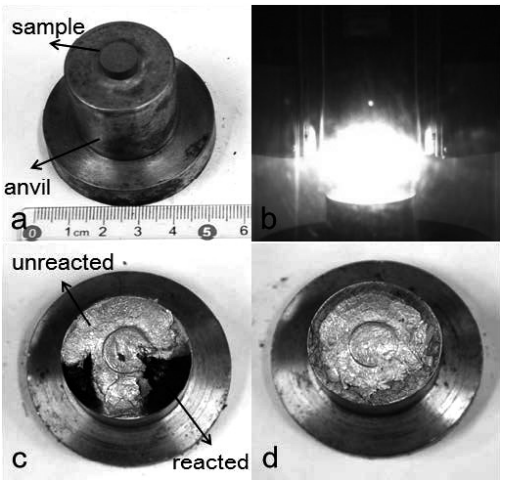

Figure 6. Impact initiated reaction of Al-PTFE in drop-weight test: (a) Al-PTFE sample placed on the anvil before the drop-weight test, (b) flame captured by high speed photography in the drop-weight test, (c) reacted Al-PTFE after a drop-weight test, (d) unreacted Al-PTFE after a drop-weight test.

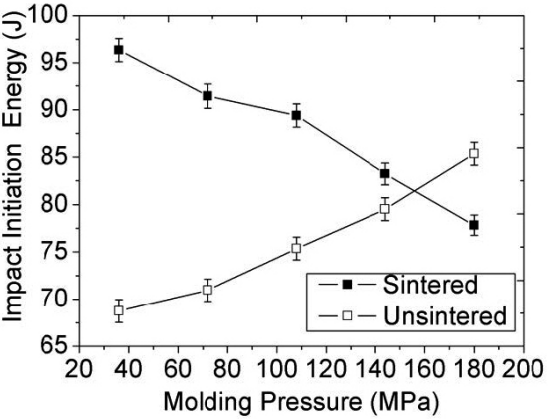

Figure 7. Plot of impact initiation energy of sintered and unsintered Al-PTFE against molding pressure (data points are average values from 25 independent tests ± the standard deviation).

The influence of sintering is consistent with the reaction mechanism of Al-PTFE. Ignition of impact-initiated reactions is triggered by the large deformation that occurs at high stress and high-strain rates. A key parameter to consider is the ability of the constituents to mix and strain simultaneously [21]. As reported in section 3.1, unsintered Al-PTFE samples are in general easier to deform and yield than sintered ones, which means unsintered Al-PTFE is more susceptible to plastic strain and fracture, and thus easier to initiate under impact. Furthermore, unsintered Al-PTFE shows clear evidence of brittleness while sintered Al-PTFE exhibits great ductility. The high ductility of sintered PTFE may therefore help cushion the Al particles from mechanical impact, thereby increasing the overall ignition energy required.

The same explanation could be applied to the influence of the molding pressure on unsintered Al-PTFE. As the molding pressure increases, the elasticity modulus and the yield stress of unsintered Al-PTFE also increase, making the constituents more difficult to strain and mix, and thus harder to initiate. This can also be confirmed by comparing the SEM images in Figures 5a and 5b, where the unsintered PTFE matrix that had been subjected to the higher molding pressure had better integrity than the one subjected to the lower molding pressure. For sintered Al-PTFE the yield stress reaches its upper limit with increasing molding pressure. Also the increased elasticity modulus has much less influence on the deformation process due to the very short elastic region compared with unsintered Al-PTFE (see Figure 1). Therefore, the impact initiation energy should either stay unchanged or be only slightly increased with increase of molding pressure. However, the initiation energy actually decreased, which indicates the existence of other influencing factors introduced by increasing the molding pressure. The most reasonable explanation could be attributed to the PTFE nanofiber networks observed in Figure 5d. It can be seen that nanofiber networks introduce many microvoids and gaps into the microstructure which are absent in Figure 5c. These microvoids and gaps could promote localized “hot-spots” with higher temperature under impact and hence accelerate the initiation. The existence of microvoids and gaps could be confirmed by the fact that PTFE nanofibers are evidence of crazing [3], which is a phenomenon that often occurs in polymers under pressure. Crazing generates microscopic gaps and microvoids because there is sufficient local stress to overcome the van der Waals force.

4 Conclusions

Quasi-static tests and drop-weight tests were performed on Al-PTFE materials. The influence of the sintering process and the molding pressure on mechanical properties and the impact initiation behavior was assessed. The conclusions derived were supported by SEM images of the microstructures of the samples discussed.

(a) The sintering process transforms Al-PTFE from a brittle material to a ductile material. The fracture strain increased from around 0.1 to above 0.7. The elastic moduli of Al-PTFE samples doubled from 108-160 MPa to 256-336 MPa and the yield stress increased from 12-16 MPa to 19-20 MPa (the upper limit of the yield stress of PTFE).

(b) Increasing the molding pressure was found to increase the elastic modulus of all the Al-PTFE samples and the yield stress of unsintered ones, because of the better integrity of the PTFE matrix and stronger interfaces between Al particles and the PTFE matrix. The sintering process makes the yield stress of PTFE approximate its upper limit regardless of changes in the molding pressure.

(c) Unsintered samples, except samples pressed under 182 MPa, required less energy to initiate than sintered samples, because the brittleness and the lower yield stress of unsintered Al-PTFE samples made them more susceptible to plastic strain and fracture.

(d) As the molding pressure was increased from 36 MPa to 182 MPa, the initiation energy for sintered Al-PTFE fell from 96 J to 68 J, whereas the initiation energy for unsintered Al-PTFE rose from 68 J to 85 J. Nanofiber networks that were observed in sintered samples produced under higher molding pressures could contribute to the opposite trends of the impact initiation energy of unsintered and sintered Al-PTFE samples.

Acknowledgements

The research was sponsored by the National Basic Research Program of China (2011CB610305) and The Open Project of State Key Laboratory (DPMEIKF 2013-06).

References

[1] Martirosyan K.S., Hobosyan M., Lyshevski S.E., Enabling Nanoenergetic Materials with Integrated Microelectronics and MEMS Platforms, *12th IEEE Int. Conf.*

Nanotechnology, Birmingham, United Kingdom, **2012**, 1-5.
[2] Zhang X., Shi A., Qiao L., Zhang J., Zhang Y.G., Guan Z.W., Experimental Study on Impact-initiated Characters of Multifunctional Energetic Structural Materials, *J. Appl. Phys.*, **2013**, *113*(8), 083508.
[3] Cai J., Walley S., Hunt R., Proud W.G., Nesterenko V.F., Meyers M.A., High-strain, High-strain-rate Flow and Failure in PTFE/Al/W Granular Composites, *Mat. Sci. Eng. A*, **2008**, *472*(1), 308-315.
[4] Nielson D.B., Tanner R.L., Lund G.K., High Strength Reactive Materials, Patent US 6 593 410, **2003**.
[5] Lund G., Nielson D., Tanner R., High Strength Reactive Materials and Methods of Making, Patent US 7 307 117, **2003**.
[6] Joshi V.S., Process for Making Polytetrafluoroethylene-aluminum Composite and Product Made, Patent US 6 547 993, **2003**.
[7] Thadhani N., Shockinduced and Shock-assisted Solid-state Chemical Reactions in Powder Mixtures, *J. Appl. Phys.*, **1994**, *76*(4), 2129-2138.
[8] Eakins D., Thadhani N.N., Shock-induced Reaction in a Flake Nickel + Spherical Aluminum Powder Mixture, *J. Appl. Phys.*, **2006**, *104*(11), 113521-113521-5.
[9] Xiong W., Zhang X.F., Wu Y., He Y., Wang C.T., Guo L., Influence of Additives on Microstructures, Mechanical Properties and Shock-induced Reaction Characteristics of Al/Ni Composites, *J. Alloys Compd.*, **2015**, *648*, 540-549.
[10] Zheng X., Curtis A.D., Shaw W.L., Dlott D.D., Shock Initiation of Nano-Al plus Teflon: Time-Resolved Emission Studies, *J. Phys. Chem. C*, **2013**, *117*(9), 4866-4875.
[11] Ames R.G., Energy Release Characteristics of Impact-initiated Energetic Materials, *Mater. Res. Soc. Symp. Proc.*, **2006**, *896*, 123-132.
[12] Eakins D., Thadhani N., Shock Compression of Reactive Powder Mixtures, *Int. Mater. Rev.*, **2009**, *54*(4), 181-213.
[13] Hunt E.M., Malcolm S., Pantoya M.L., Davis F., Impact Ignition of Nano and Micron Composite Energetic Materials, *Int. J. Impact Eng.*, **2009**, *36*(6), 842-846.
[14] Ames R., Vented Chamber Calorimetry for Impact-Initiated Energetic Materials, *43rd AIAA Aerospace Sciences Meeting and Exhibit*, Reno, USA, **2005**.
[15] Lee R.J., Mock W. Jr., Carney J.R., Holt W.H., Pangilinan G.I., Gamache R.M., Boteler J.M., Bohl D.G., Drotar J., Lawrence G.W., Reactive Materials Studies, *AIP Conf. Proc.*, **2006**, *845*, 169-174.
[16] Casem D.T., Mechanical Response of an Al-PTFE Composite to Uniaxial Compression Over a Range of Strain Rates and Temperatures, DTIC Document, **2008**.
[17] Raftenberg M., Mock W. Jr., Kirby G., Modeling the Impact Deformation of Rods of a Pressed PTFE/Al Composite Mixture, *Int. J. Impact Eng.*, **2008**, *35*(12), 1735-1744.
[18] Cai J., Properties of Heterogeneous Energetic Materials Under High Strain, High Strain Rate Deformation, *Dissertation Abstracts International*, **2007**, *68*(07), 4758.
[19] Xu S., Yang S., Zhang W., The Mechanical Behaviors of Polytetrafluorethylene/

Al/W Energetic Composites, *J. Phys. Condens. Matter.*, **2009**, *21*(28), 285401.
[20] Wei D., Dave R., Pfeffer R., Mixing and Characterization of Nanosized Powders: An Assessment of Different Techniques, *J. Nanopart. Res.*, **2002**, *4*(1-2), 21-41.
[21] Cheng J.L., Hng H.H., Lee Y.W., Du S.W., Thadhani N.N., Kinetic Study of Thermal- and Impact-initiated Reactions in Al–Fe_2O_3 Nanothermite, *Combust. Flame*, **2010**, *157*(12), 2241-2249.
[22] Lomov I., Herbold E., Mesoscale Studies of Mixing in Reactive Materials During Shock Loading, *AIP Conf. Proc.* **2012**, *1426*, 733-736.
[23] Mason B.A., Groven L.J., Son S.F., The Role of Microstructure Refinement on the Impact Ignition and Combustion Behavior of Mechanically Activated Ni/Al Reactive Composites, *J. Appl. Phys.*, **2013**, *114*(11), 113501.
[24] Yarrington C.D., Combustion Characterization and Modeling of Novel Energetic Materials: Si/PTFE/Viton and Al/PTFE/Viton, ProQuest, UMI Dissertations Publishing, **2011**.
[25] Callister W.D.J., *Fundamentals of Materials Science and Engineering*, John Wiley & Sons, **2008**; ISBN 978-0-521-86675-0.